

## Leakage current behavior in pulsed laser deposited Ba ( Zr 0.05 Ti 0.95 ) O 3 thin films

Amab Mukherjee, P. Victor, J. Parui, and S. B. Krupanidhi

Citation: *Journal of Applied Physics* **101**, 034106 (2007); doi: 10.1063/1.2433717

View online: <http://dx.doi.org/10.1063/1.2433717>

View Table of Contents: <http://scitation.aip.org/content/aip/journal/jap/101/3?ver=pdfcov>

Published by the [AIP Publishing](#)

---

### Articles you may be interested in

[Temperature-dependent leakage current behavior of epitaxial Bi<sub>0.5</sub>Na<sub>0.5</sub>TiO<sub>3</sub>-based thin films made by pulsed laser deposition](#)

*J. Appl. Phys.* **110**, 103710 (2011); 10.1063/1.3660428

[Electrical conduction transition and largely reduced leakage current in aluminum-doped barium strontium titanate thin films heteroepitaxially grown on Ir/MgO/Si \( 100 \)](#)

*Appl. Phys. Lett.* **86**, 132902 (2005); 10.1063/1.1896448

[Leakage current conduction of pulsed excimer laser ablated BaBi<sub>2</sub>Nb<sub>2</sub>O<sub>9</sub> thin films](#)

*J. Appl. Phys.* **92**, 415 (2002); 10.1063/1.1473216

[Microstructure related influence on the electrical properties of pulsed laser ablated \(Ba,Sr\)TiO<sub>3</sub> thin films](#)

*J. Appl. Phys.* **88**, 3506 (2000); 10.1063/1.1288018

[Leakage current of sol-gel derived Pb\(Zr,Ti\)O<sub>3</sub> thin films having Pt electrodes](#)

*Appl. Phys. Lett.* **75**, 3411 (1999); 10.1063/1.125310

---



**Not all AFMs are created equal**  
**Asylum Research Cypher™ AFMs**  
**There's no other AFM like Cypher**

[www.AsylumResearch.com/NoOtherAFMLikeIt](http://www.AsylumResearch.com/NoOtherAFMLikeIt)

**OXFORD**  
INSTRUMENTS  
*The Business of Science®*

# Leakage current behavior in pulsed laser deposited $\text{Ba}(\text{Zr}_{0.05}\text{Ti}_{0.95})\text{O}_3$ thin films

Arnab Mukherjee,<sup>a)</sup> P. Victor,<sup>b)</sup> J. Parui, and S. B. Krupanidhi  
*Materials Research Center, Indian Institute of Science, Bangalore 560012, India*

(Received 13 November 2005; accepted 28 November 2006; published online 7 February 2007)

Barium zirconium titanate [ $\text{Ba}(\text{Zr}_{0.05}\text{Ti}_{0.95})\text{O}_3$ , BZT] thin films were prepared by pulsed laser ablation technique and dc leakage current conduction behavior was extensively studied. The dc leakage behavior study is essential, as it leads to degradation of the data storage devices. The current-voltage ( $I$ - $V$ ) of the thin films showed an Ohmic behavior for the electric field strength lower than 7.5 MV/m. Nonlinearity in the current density-voltage ( $J$ - $V$ ) behavior has been observed at an electric field above 7.5 MV/m. Different conduction mechanisms have been thought to be responsible for the overall  $I$ - $V$  characteristics of BZT thin films. The  $J$ - $V$  behavior of BZT thin films was found to follow Lampert's theory of space charge limited conduction similar to what is observed in an insulator with charge trapping moiety. The Ohmic and trap filled limited regions have been explicitly observed in the  $J$ - $V$  curves, where the saturation prevailed after a voltage of 6.5 V referring the onset of a trap-free square region. Two different activation energy values of 1.155 and 0.325 eV corresponding to two different regions have been observed in the Arrhenius plot, which was attributed to two different types of trap levels present in the film, namely, deep and shallow traps. © 2007 American Institute of Physics. [DOI: 10.1063/1.2433717]

## I. INTRODUCTION

Ferroelectrics thin films with high dielectric constant and low leakage current are important in fabricating capacitor cells of gigabit dynamic random access memories (DRAMs).<sup>1-3</sup> Barium titanate related thin films, such as barium strontium titanate [ $(\text{Ba}_{1-x}\text{Sr}_x)\text{TiO}_3$  (BST)], barium zirconium titanate [ $\text{Ba}(\text{Zr}_x\text{Ti}_{1-x})\text{O}_3$  (BZT)], and barium stannous titanate [ $\text{Ba}(\text{Sn}_x\text{Ti}_{1-x})\text{O}_3$ ] are the leading materials that have attracted great attention in recent years for their significant applications<sup>4-7</sup> in this field. Among various materials, BST has attracted the most attention because of its high dielectric constant, low leakage current, and low dielectric dispersion. However, the limitation of BST thin films is that they have a very high leakage current behavior at low electric field,<sup>8</sup> which in turn limits the thickness of the film and electrode area of the capacitor. Among the other materials, which have been recognized as substitute of BST, BZT seems to be a promising material to solve the recent problems. Though the substitution of Ti by Zr induces a reduction in the average grain size and decreases the dielectric constant ( $\epsilon_r$ ), it maintains low leakage current<sup>9-11</sup> and becomes more stable against thermal degradation as compared to BST thin films.

The performance of the data storage devices depends on their ability to retain stored charges of the corresponding materials, which in turn stores the information in terms of charges. Various issues such as polarization switching, fatigue, and imprint have been extensively investigated for

many other ferroelectric materials before integrating them in miniaturized circuits. Another significant feature, which is very important for the quality and the reliability of the ferroelectric devices, is low leakage current. Particularly, for thin films, where a nominal voltage across the sample produces a very high electric field, the mechanism of charge transport becomes very complicated and crucial. Not many studies are done on the conduction behavior of thin films of  $\text{Ba}(\text{Zr}_{0.05}\text{Ti}_{0.95})\text{O}_3$  (BZT), while it is believed that high leakage current is responsible for polarization degradation of ferroelectric memory devices.<sup>12</sup> It is therefore essential to have an insight of charge transport mechanism in BZT thin film under a dc electric field. There are several proposed mechanisms, which explain charge transport phenomena at high and low electric fields.<sup>13-15</sup> Conduction mechanism inside a BZT thin film will depend on distribution of charge traps, which are inevitably present within any real sample.<sup>16</sup> In this article, we have presented the results of dc conduction measurements on thin films of BZT that were prepared by a laser deposition process.

## II. EXPERIMENT

Pulsed laser ablation was used to deposit thin films of BZT, due to its advantage in terms of good stoichiometric control, faster growth rate, and ease of control. In the present work  $\text{Ba}(\text{Zr}_{0.05}\text{Ti}_{0.95})\text{O}_3$  thin films were deposited using this technique. The target used for this purpose was well-sintered stoichiometric ceramic pellet of  $\text{Ba}(\text{Zr}_{0.05}\text{Ti}_{0.95})\text{O}_3$ . A 248 nm KrF pulsed laser operating at a repetition rate of 5 Hz and a fluence of 3 J/cm<sup>2</sup> was used for the fabrication of these films. The oxygen pressure in the deposition chamber was kept at 100 mTorr with substrate temperature at 675 °C. Thus, the films were annealed inside the deposition chamber itself. Hence, the films obtained were *in situ* crystallized. The

<sup>a)</sup> Author to whom correspondence should be addressed; present address: Department of Chemistry, Rice University, Texas; electronic mail: arnab123@rice.edu

<sup>b)</sup> Present address: Materials Science and Engineering Department, Rensselaer Polytechnic Institute, Troy, New York 12180.

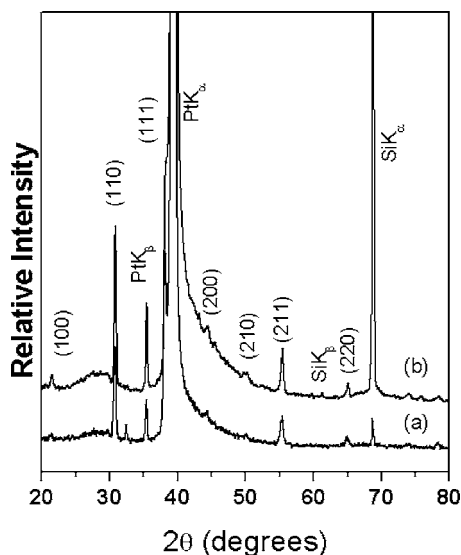


FIG. 1. X-ray diffraction plots of BZT thin films (a) as deposited and *in situ* annealed at 650 °C (b) annealed at 675 °C at 100 mTorr oxygen pressure for 30 min on Pt (111) coated Si substrates.

films were deposited on Pt (111)/TiO<sub>2</sub>/SiO<sub>2</sub>/Si substrates. Crystallinity and phase purity have been confirmed using x-ray diffraction and microstructural analysis has been carried out using scanning electron microscopy (SEM). Using cross sectional SEM we have confirmed the film thickness near 0.41 μm. The composition of the film was confirmed using Energy dispersive analysis of x rays (EDAXs). Gold dots of 500 μm diameters were deposited using thermal evaporation on the top of the film for electrical measurements.

### III. RESULTS AND DISCUSSION

#### A. Structural characterization

In Fig. 1, x-ray diffraction (XRD) study shows the temperature effect on crystallization of *in situ* grown BZT thin films. From the XRD plot it is clear that the film has perovskite structure.<sup>17</sup> Between the two XRD plots, it is clearly seen that 650 °C annealed films are [110] oriented whereas 675 °C annealed films have come out as multioriented. We have studied the growth of films at annealing temperatures 400, 500, and 600 °C, but they are amorphous in nature. Hence, according to our study of *in situ* growth of BZT thin films, we can say that their crystallization starts above 600 °C for the particular deposition condition stated in the Experiment section.

#### B. dc leakage behavior of Ba(Zr<sub>0.05</sub>Ti<sub>0.95</sub>)O<sub>3</sub> thin films on Pt [111] substrate

Leakage current behavior is supposed to be an important part in the study of dielectric thin films. As BZT thin films can be used as a capacitor material in DRAMs, correlation of processing and properties has a definite impact in improving device properties and costs. When a voltage is applied to a ferroelectric capacitor, the current flowing through the external circuit comprises of two components, polarization contribution and leakage contribution. The polarization current

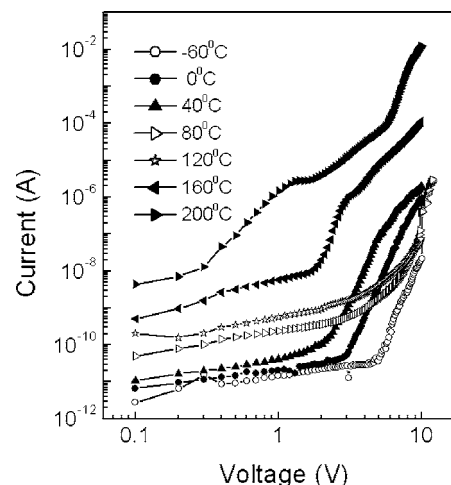


FIG. 2. dc leakage current vs voltage behavior of BZT thin films at different temperatures.

shows a transient behavior until certain time and might contribute to the overall response of current voltage (*I-V*) behavior if the measurements are taken within the transient time.<sup>18</sup>

To perceive any interference of the transient response into the measured value we have performed the *I-V* measurements at different delay times (time delay between the change of voltage and acquisition of data), namely, 10, 50, and 100 ms. The result did not show any significant change, confirming that the experimentally measured current for 100 ms delay time was the true leakage behavior of the sample. Hence, all further measurements were done with a delay time of 100 ms. Here, it is noteworthy that a detail analysis of transient response and leakage current of dielectric thin films was reported earlier by Dietz and Waser.<sup>18</sup>

Figure 2 shows the variation in leakage current versus applied voltage at different temperatures, varying from -60 to 200 °C. Different conduction mechanisms such as Schottky<sup>12</sup> and space charge limited conduction<sup>19</sup> (SCLC) have been verified to explain the true nature of charge transport phenomenon in BZT thin films. Leakage current is seen to begin with a linear dependence with voltage, as it is evident from its slope in the log-log plot. After a voltage of 3 V and above, the slope of the *I-V* curve has increased up to a value about 9–13 and then has come down to a value of 4.5 referring the saturation above a voltage of 6.5 V. The sudden initial increase of current in the *I-V* plot was obtained repetitively, which ruled out the possibility of breakdown phenomenon in the applied voltage range to be the reason for sudden increase of current above 3 V. Each plot shows a change in the leakage current characteristic with an increase in temperature. There are certain other facts recognized along with the increase in leakage current with respect to applied voltage as well as temperature. Among the other facts, the change in trap filled linear voltage ( $V_{TFL}$ ) is the most noticeable fact. The voltage corresponding to  $V_{TFL}$  is found to shift towards lower values as the temperature is raised from -60 to 40 °C, but this voltage seems to rise to higher values as we go to higher temperatures. Apparently a lowering of  $V_{TFL}$  value is again observed at very high temperatures starting from 100 °C. The detail explanation has been noted in Sec. III C.

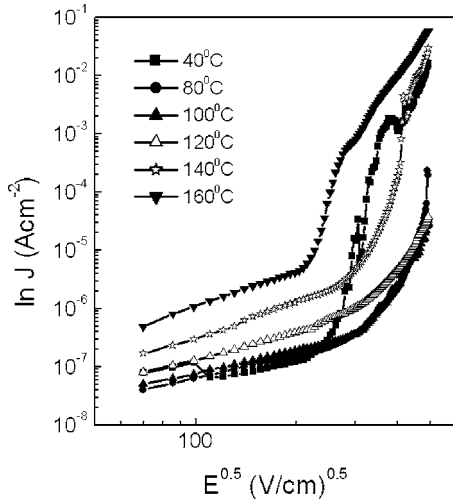


FIG. 3.  $\ln J$  vs  $E^{0.5}$  plot of BZT thin films at various temperatures to examine Schottky-type conduction mechanism.

The observed  $I$ - $V$  behavior may be due to electrode-limited processes such as Schottky-type conduction or may be due to bulk-limited conduction such as space charge limited conduction (SCLC). Schottky emission mechanism is an electrode-limited conduction, where the Schottky barrier generated at the interface of the electrode and film dominates the entire leakage current. The electrode-limited current density (so called Schottky current density) upon application of an electric field behaves according to the following equation:

$$J \propto T^2 \exp[-(\phi_0 - \beta E^{1/2})/\kappa T], \tag{1}$$

where “ $\phi_0$ ” is the work function difference between the metal and the insulator, “ $\beta$ ” is a constant given by

$$\beta = \frac{e^3}{\pi \epsilon_0 K}, \tag{2}$$

$K$  denotes the high frequency dielectric constant of the sample.

To check for the Schottky emission theory, we plotted current density ( $J$ ) as a function of electric field ( $E^{1/2}$ ) in semilog scale, which is shown in Fig. 3.

The expression for current density should give rise to a linear graph for the above plot if Schottky conduction mechanism is followed. But nonlinearity was observed in the high field region ( $>7.5$  MV/m). So concentrating only in the lower field region, where the curves seem to be straight lines, the high frequency dielectric constant was calculated for  $\ln J$  vs  $E^{1/2}$  at 100 °C, as shown in Fig. 4. The slope of this straight line must be equal to  $\beta/\kappa T$ , from where the  $\beta$  value was obtained, and the calculated dielectric constant from the  $\beta$  value should match well with the high frequency dielectric constant.

The calculated dielectric constant and refractive index ( $\epsilon_r = n^2$ ) values are 0.12 and 0.35, respectively, which are one order less than the expected values for dielectric constant and refractive indices for BZT thin films. The expected high frequency dielectric constant ( $\epsilon_r$ ) for BZT thin films is 100.

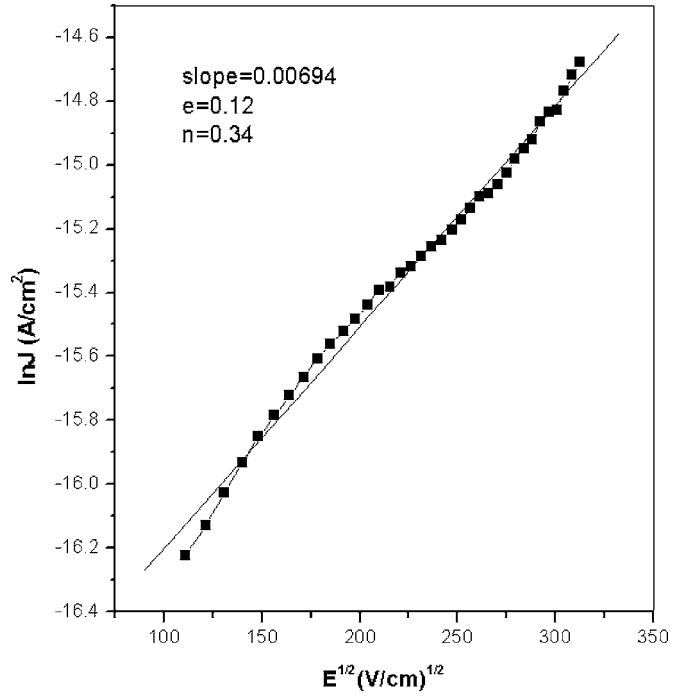


FIG. 4. Plot of  $\ln J$  vs  $E^{0.5}$  of BZT thin films measured at 100 °C.

Hence, the nonlinear nature of the curve and highly different dielectric constant values rules out the possibility of Schottky-type conduction.

Secondly, the temperature dependence of the  $I$ - $V$  curve was also compared with that of Schottky-type conduction. It is evident from Eq. (1) that the exponent of the equation should decrease with increase in electric field at all temperatures. But the Arrhenius plot of  $\ln(J/T^2)$  vs  $1000/kT$  shown in Fig. 5 depicts an increase in activation energy with voltage, which is contrary to the expected result. Activation energy values have been calculated from the slope of the curves obtained by linear fitting. So this phenomenon also discards the Schottky-type conduction. These two verifications disqualify the Schottky-type conduction and, hence, the possibility of Schottky emission controlled conduction was ruled out.

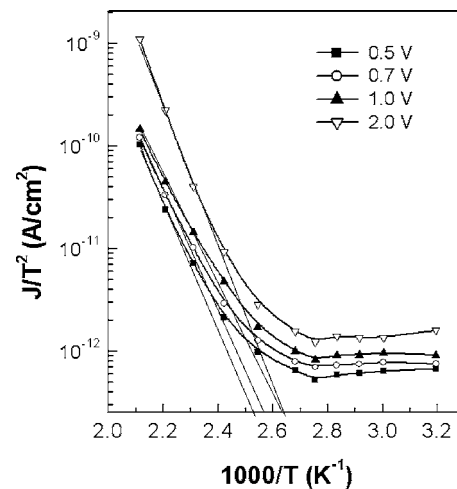


FIG. 5. Arrhenius plot for BZT thin films at different voltages.

Then the charge transport behavior inside BZT thin films may be described by the theory suggested by Lampert and Mark,<sup>20</sup> for space charge limited current in insulators. Considering a SCLC mechanism in our films, the shift in the  $V_{TFL}$  can be assumed as a direct indication of its validity. The space charge limited conduction has explained better what is observed in  $I$ - $V$  characteristics. A pure SCLC should exhibit square law dependence at high electric field, where  $I$ - $V$  plot in log-log scale will appear as a straight line with a slope of 2. According to SCLC mechanism, in a typical  $I$ - $V$  plot there should be a region where the current varies as square of the applied voltage and this region of the plot is defined as “trap-free square” region. However, this behavior can be modified in the presence of the bulk-generated charges in the sample, as the thermally excited valence band electrons or the presence of free electrons due to oxygen vacancies can take part in the conduction mechanism. These electrons may completely screen the effect of the excess injected charge from the electrode. This is worthy to note that space charge conduction arises due to excess charge injection from the electrode in the sample. As long as the number of injected charge does not exceed the number of charge carriers already existing in the sample, the effect of space charge will not be observed. Hence, the bulk generated charge carrier would give rise to linear  $I$ - $V$  characteristic. In the case of SCLC, the linear region extends up to a certain voltage, known as the crossover voltage, where there is an abrupt rise in the magnitude of the current and after this region the current value saturates and varies with the voltage as power law:

$$I \propto V^2, \quad (3)$$

defined as “Child’s square law.”

However, in our samples, we suspect that there are several trap sites, which capture the injected electrons and prevent them from showing the space charge effect. In general, there are two types of traps: the traps above the Fermi level are the shallow traps and the traps below the Fermi level are the deep traps. As the Fermi-Dirac (FD) distribution function, which describes the probability to occupy an energy level, has a value less than the unity above Fermi level, during charge trapping both deep and shallow traps will be partially empty.

However, the deep traps would get completely filled at trap filled limit voltage ( $V_{TFL}$ ). Beyond this voltage, all the excess charges would be injected into the conduction band, for which there will be an enormous increase in current with applied voltage. For a set of traps distributed in energy, the increase in current would be less abrupt and would follow

$$I \sim V^\alpha, \quad (4)$$

until it shows a trap-free square region.

For our measurements, the linear region extended up to a voltage of 3 V, after which, it was found that the current showed an abrupt increase following the power law with an exponent  $\alpha \approx 13$ , and after this region there is a saturation zone, which had a slope  $\sim 4$ . These three regions formed a triangle called the Lampert triangle.<sup>21</sup> But we were not able to see a trap-free square region, as the applied voltage may

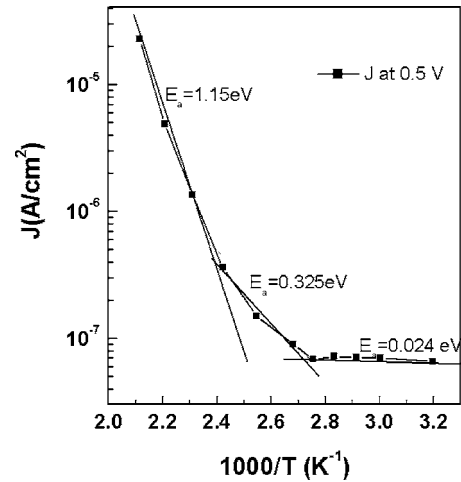


FIG. 6. Arrhenius plot of BZT thin films measured at 0.5 V in order to calculate the activation energy values of trap levels.

not be sufficient to show saturation, and we were not able to supply still higher voltages as that was causing the breakdown of the film.

### C. Trap filled voltage

We have analyzed our measurements obtained from the current-voltage characteristics with variation in ambient temperature in their respective Arrhenius plots. Figure 6 shows the  $\ln J$  vs  $1000/T$  plots for the BZT thin films. The current in the linear region has been found to fit with the Arrhenius equation:

$$\ln J = \ln J_0 - (E_a/k \times 1000)(1000/T), \quad (5)$$

where  $J$  is the current density,  $E_a$  is activation energy of the charge carriers to participate in the conduction process,  $k$  is Boltzman’s constant, and  $T$  is temperature in Kelvin scale. Here  $J_0$  is the intrinsic current density of the sample.

We have calculated the activation energy equating the slope of the plots (shown in Fig. 6) with  $(E_a/k \times 1000)$ . It has been found to have two distinctly different regions, one region has an activation energy ( $E_a$ ) value of 1.155 eV and the other one has 0.325 eV. These values consolidate the fact that there are two distinctly different types of trap levels existing in our films, namely, the deep and shallow traps. As deep traps are the one with higher activation energy and the shallow traps are the ones with lower energy values,<sup>15</sup> in our case the first region is related to deep level traps whereas the other region is due to shallow traps. Though we have already raised the issue earlier in Sec. III B, to explain it clearly, in Fig. 7, the variation of trap filled voltage ( $V_{TFL}$ ) of BZT films is shown as a function of temperature. It is observed that from room temperature to 100 °C the  $V_{TFL}$  exhibits an increasing trend, but above 100 °C, it shows a decreasing trend up to 200 °C. Beyond 200 °C it was not possible to carry out further experiment due to electrode damaging. But the phenomenon can be explained by space charge theory. According to the space charge theory, the space charges are represented by their equilibrium distribution, which is identical to Fermi-Dirac distribution function, at all temperatures. But to achieve the equilibrium a certain time is required. The

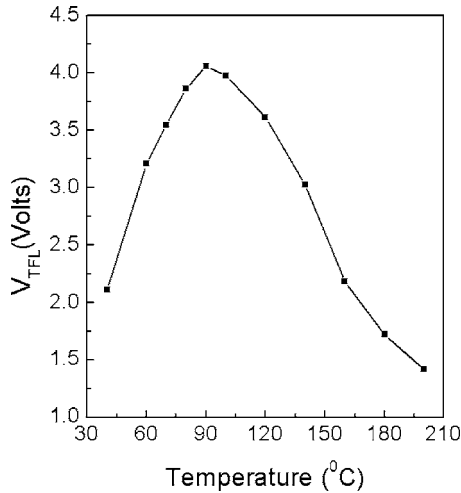


FIG. 7. Variation of  $V_{TFL}$  of BZT thin films shown with respect to temperature.

charges, immediately after being injected into the sample, have to equilibrate with the surrounding, to reach the time independent distribution of electrons amongst various energy levels. This has to occur throughout the entire sample. For that, the electrons have to migrate uniformly through the sample, so that they could seek equilibrium trap sites. This means that space charge transient would govern the phenomenon of the trap distribution if observed in a short time scale. It is known that the space charge transient in thin films could be of a time scale of several seconds depending upon the sample. The electron distribution would therefore be limited by the competition between the rate of trapping and detrapping of electrons. The trapping rate would be represented by

$$T_{E_c \rightarrow E_t} = N(E_c)\sigma(E_t)N(E_t), \quad (6)$$

where  $T$  represent the rate of transition between the energy states mentioned in the suffices,  $N$  represents the density of unoccupied energy states at energy  $E$ , and  $\sigma(E_t)$  is the capture cross section of the traps.

The detrapping of electrons would be given by

$$T_{E_t \rightarrow E_c} = \nu XN(E_t)\exp(-\Delta E/kT)N(E_c), \quad (7)$$

where the energy difference has been denoted by  $E$  and the attempt frequency to escape is  $\nu$ .

At a lower temperature, there would be very few electrons in the upper energy state (from where it is captured to the trapped sites), and trapping rate also would not change much with temperature. Therefore, the entire process would be limited by the detrapping of electrons only. If the temperature was increased, few of the filled traps would reemit some electrons from the trap sites, and again those sites would become empty. The ratio of the free electron to the trapped electrons would increase with temperature. As a result, one would have to apply a higher voltage to inject further electrons into the sample, so that all the trap levels get filled with electrons. This explains the rise in  $V_{TFL}$  value from room temperature to 100 °C. Therefore we can say the value of trap filled voltage was found to increase according to Lampert's space charge law.<sup>16</sup>

But at higher temperature there would be significant amount of electrons in the conduction band (due to thermal generations), which in turn would increase the rate of trapping, causing a greater number of trapped electrons. There would be contribution from detrapping also, but the increased rate of trapping might overcome the detrapping rate at higher temperature. Therefore, it is expected that the number of electrons required to fill all the traps would be less at a higher temperature than it was at lower temperature. This might bring down the trap filled voltage closer to the actual lower values.<sup>16,22</sup> In our samples, above phenomenon is seen to be prominent above 100 °C. However, this can saturate at the equilibrium value of  $V_{TFL}$ . It has been seen that the reduction of  $V_{TFL}$  exhibits a saturating trend after 180 °C.

#### IV. CONCLUSIONS

In this present paper, we have analyzed the leakage current behavior of BZT thin films at different temperatures. We have ruled out the possibility of Schottky emission controlled conduction and explained the phenomena with SCLC. The  $I$ - $V$  characteristics have been seen to follow Lampert's theory of SCL conduction. Ohmic and trapped filled limited regions have been clearly observed in the  $I$ - $V$  characteristics. A perfect "trap-free square" region has not been observed because of breakdown voltage, but considerable amount of saturation at higher voltages indicates the fact that "Child's law" might have been followed at higher voltages. Existence of both shallow and deep traps has been found to be present in the sample within the experimental conditions. The trap energies calculated from the  $J$ - $T$  characteristics were found to be 0.325 and 1.155 eV for the shallow and deep traps, respectively. The onset voltage ( $V_{TFL}$ ) of the trap filled limited region in the  $I$ - $V$  curve has showed an increasing and decreasing trend with temperature and that behavior of  $V_{TFL}$  has been explained considering the dynamical equilibrium between thermally generated and injected charge carriers.

<sup>1</sup>T. Sumi *et al.*, Jpn. J. Appl. Phys., Part 1 **35**, 1516 (1996).

<sup>2</sup>T. Kaga, M. Ohkura, F. Murai, N. Yokoyama, and E. Takeda, J. Vac. Sci. Technol. B **13**, 2329 (1995).

<sup>3</sup>H. Achard and H. Mace, *Science and Technology of Electroceramic Thin Films*, edited by O. Auciello and R. Waser (Kluwer, Dordrecht, 1994).

<sup>4</sup>K. Abe and S. Komatsu, J. Appl. Phys. **77**, 6461 (1995).

<sup>5</sup>T. Nakamura, Y. Yamanaka, A. Morimoto, and T. Shimizu, Jpn. J. Appl. Phys., Part 1 **34**, 5150 (1995).

<sup>6</sup>T. Kuroiwa, Y. Tsunemine, T. Horikawa, T. Makita, J. Tanimura, N. Mikami, and K. Sato, Jpn. J. Appl. Phys., Part 1 **33**, 5187 (1994).

<sup>7</sup>C. M. Wu and T. B. Wu, Jpn. J. Appl. Phys., Part 1 **36**, 1164 (1997).

<sup>8</sup>K. Numata, Y. Fukuda, K. Aoki, and A. Nishimura, Jpn. J. Appl. Phys., Part 1 **34**, 5245 (1995).

<sup>9</sup>S. Hoffman and R. Waser, Integr. Ferroelectr. **17**, 141 (1997).

<sup>10</sup>C. M. Wu, T. B. Wu, and M. L. Chen, Appl. Phys. Lett. **69**, 2659 (1996).

<sup>11</sup>D. Hennings and A. Schnell, J. Am. Ceram. Soc. **65**, 539 (1982).

<sup>12</sup>C. Alemany, R. Jimenez, J. Revilla, J. Mendiola, and M. L. Calzada, J. Phys. D **32**, L79 (1999).

<sup>13</sup>W. Schottky, Z. Phys. **113**, 367 (1939).

<sup>14</sup>J. Frenkel, Phys. Rev. **54**, 647 (1938).

<sup>15</sup>N. F. Mott, and R. W. Gurney, *Electronic Processes in Ionic Crystals*, 2nd ed. (Oxford University Press, Flair Lawn, NJ, 1948), Vol. V.

<sup>16</sup>S. Bhattacharyya, A. Laha, and S. B. Krupanidhi, J. Appl. Phys. **91**, 4543 (2002).

<sup>17</sup>F. M. Pontes, M. T. Escote, C. C. Escudeiro, E. R. Leite, E. Longo, A. J. Chiquito, P. S. Pizani, and J. A. Varela, *J. Appl. Phys.* **96**, 4386 (2004).

<sup>18</sup>G. W. Dietz and R. Waser, *Integr. Ferroelectr.* **9**, 327 (1995).

<sup>19</sup>M. A. Lampert, *Phys. Rev.* **103**, 1648 (1956).

<sup>20</sup>M. A. Lampert and P. Mark, *Current Injection in Solids* (Academic, New York, 1970).

<sup>21</sup>J. F. Scott, *Ferroelectr. Rev.* **1**, 62 (1998).

<sup>22</sup>A. Laha and S. B. Krupanidhi, *J. Appl. Phys.* **92**, 415 (2002).